Applied Mathematical Sciences, Vol. 19, 2025, no. 6, 249 - 269
HIKARI Ltd, www.m-hikari.com
https://doi.org/10.12988/ams.2025.919261

Spatio-Temporal Cooperative Guidance Law for Loitering Munitions Based on Adaptive Sliding Mode Control

Zetian Zhang and Min Gao

Shijiazhuang Campus of Army Engineering University
Shijiazhuang 050000, Hebei, China

Abstract

This paper addresses the multi-constraint guidance problem in the cooperative strike of loitering munitions against targets and proposes a distributed spatio-temporal cooperative guidance law based on adaptive sliding mode control. This guidance law simultaneously considers three types of constraints—time coordination, impact angle coordination, and attack azimuth coordination—constructing a unified control framework. By designing a non-singular terminal sliding mode surface combined with an adaptive robust term, it effectively suppresses system chattering and enhances robustness against target maneuvers and external disturbances. Notably, a dynamic azimuth allocation strategy based on target velocity is proposed, which adaptively adjusts the spatial distribution formation of the loitering munitions according to the target's speed, enabling dynamic encirclement or tail-chase attacks against the target. Simulation results demonstrate that the proposed guidance law achieves high-precision time synchronization, impact angle control, and azimuth distribution under different target velocity conditions, while the control effort remains within the practical overload limits of loitering munitions, indicating strong engineering applicability and tactical flexibility.

Keywords: loitering munition, cooperative guidance, time cooperation, impact angle cooperation, attack azimuth cooperation

1 Introduction

Loitering munitions, which combine both reconnaissance and strike capabilities, are a new type of intelligent ammunition. Their primary targets include fortifications, armored vehicles, and other key infrastructure, and they have been extensively deployed in regional conflicts such as the Nagorno-Karabakh conflict, the Russia-Ukraine conflict, and the Yemeni civil war [1]. To enhance the effectiveness of loitering munitions and improve the probability of target destruction and strike accuracy, the inter-missile communication capability can be utilized to enable multi-missile cooperative attacks through the exchange of guidance information. Coordination in such systems can generally be categorized into temporal constraints and spatial constraints, with spatial constraints further subdivided into impact angle constraints and attack azimuth constraints. As the complexity of battlefield environments increases and the diversity of targets expands, relying solely on temporal or spatial coordination is no longer sufficient to meet the requirements of cooperative strikes. Consequently, the development of multi-constraint spatiotemporal cooperative guidance laws, which integrate both temporal and spatial constraints, has become the mainstream research direction [2–3].

Given the relatively limited computational capability of loitering munitions, adopting a "leader-follower" centralized cooperative architecture is a more convenient method to achieve multi-missile coordination. Reference [5] proposes a two-layer cooperative architecture: the upper layer coordinates temporal cooperation by using remaining time as a coordination variable, while the lower layer relies on the terminal guidance laws of individual loitering munitions to achieve strikes with specified timing and attack direction. However, this approach suffers from significant system redundancy and weak fault tolerance, such that the failure of a critical node may lead to the collapse of overall coordination. Reference [6] constructs a linearized motion model based on optimization theory and linearization assumptions, integrating terminal miss distance, impact angle, and energy consumption into an optimal guidance problem. This method reduces missile overload, but it imposes a high computational burden, demanding substantial processing power from onboard computers. Reference [7] introduces an underactuated three-dimensional cooperative guidance law based on consensus theory for fixed targets. However, this method is highly sensitive to communication performance and is prone to interference.

Recently, distributed cooperative guidance laws based on adaptive sliding mode control theory have gained prominence due to their high robustness and rapid convergence speed. However, sliding mode control is susceptible to chattering phenomena and typically requires larger control efforts [8–14]. Reference [15] proposes a two-layer cooperative guidance law for the line-of-sight direction and its normal vector, designed using terminal sliding mode control to mitigate chattering induced by the sign function. Despite this, the method is constrained by finite-time convergence, with convergence time being dependent on initial conditions, thus limiting its suitability for terminal guidance with short response

times. In response, Reference [16] designs a spatiotemporal-constrained distributed cooperative guidance law, employing fixed-time stability theory and adaptive sliding mode control. However, the desired terminal angles are predefined and cannot dynamically adjust the missile swarm's spatial distribution according to the evolving battlefield situation, thereby restricting tactical flexibility. References [17–20] apply differential game theory to derive cooperative guidance laws by incorporating performance metrics such as energy constraints, interception angle constraints, and miss distance, and addressing linear dynamics of arbitrary order. While these methods hold promise, they require high computational power on the missile's onboard platform and rely on idealized models, which pose challenges to practical implementation.

It is noteworthy that the aforementioned studies either do not consider attack azimuth constraints or only address inter-missile collision avoidance, without addressing the scenario in which multiple missiles surround and attack a target from various directions. In fact, with the advancement of swarm warfare theory, loitering munitions launched from a fixed position often strike a target from only a limited set of azimuths around it. This leads to a failure in creating an effective encirclement and attacking from multiple directions simultaneously. Therefore, it is imperative to incorporate attack azimuth constraints, enabling missile swarms to adjust their encirclement posture based on target characteristics and achieve more effective target capture.

In this paper, adaptive sliding mode control theory is employed to integrate temporal constraints, impact angle constraints, and attack azimuth constraints into a unified framework. A distributed control strategy is proposed, wherein inter-missile communication is used to coordinate guidance parameters. Moreover, an adaptive dynamic distribution strategy based on target velocity is introduced, which allows the missile swarm to self-adjust its formation in response to the target's speed. The effectiveness of the proposed guidance law is rigorously verified through Lyapunov stability analysis and simulation experiments.

2 Loitering Munition Cooperation Model

To facilitate the description of the relative position relationship between the loitering munition and the target, the following coordinate systems are first defined:

1) Ground Inertial Coordinate System $Oxyz$

The target position is the origin O. The Ox axis lies in the ground plane, pointing directly ahead of the target. The Oy axis lies in the ground plane, perpendicular to Ox, with the positive direction being a 90-degree clockwise rotation from the Ox axis. The Oz axis points skyward, perpendicular to the ground plane, with upward being positive.

2) Spherical Coordinate System $Or\phi\theta$

The target position is the origin O. r is the distance of the line-of-sight (LOS), positive from the origin towards the munition. ϕ is the elevation angle of the muni-

tion relative to the target, positive upward from the horizontal plane. θ is the azimuth angle of the munition relative to the target, measured clockwise from the target's velocity vector direction, ranging from 0 to 2π.

The relative position vector in the ground inertial coordinate system is represented as $\boldsymbol{r} = [x, y, z]^T$, where x, y, z are the components in the three directions.

The rate of change of the LOS distance is the difference in the velocities of the munition and target projected onto the LOS direction. Under the simplified assumption that the munition's body axis aligns with its velocity direction, it can be expressed as:

$$\dot{\boldsymbol{r}} = -\boldsymbol{V}_M \cos\theta \cos\phi + \boldsymbol{V}_T \cos\theta_T \cos\phi_T \tag{1}$$

The change in azimuth angle is caused by the difference in tangential velocities. Its rate of change is calculated as:

$$\boldsymbol{r}\dot{\theta} = \boldsymbol{V}_M \sin\theta - \boldsymbol{V}_T \sin\theta_T + a_\theta \tag{2}$$

The rate of change of the elevation angle is:

$$\boldsymbol{r}\dot{\phi}\cos\theta = -\boldsymbol{V}_M \sin\phi + \boldsymbol{V}_T \sin\phi_T + a_\phi \tag{3}$$

In the above equations, $\boldsymbol{a}_\theta$ and $\boldsymbol{a}_\phi$ are the normal acceleration commands.

3 Cooperative Guidance Law Design

3.1. Time Cooperative Controller

The objective of time cooperation is to make the remaining flight time (Time-to-Go, tgo) of all loitering munitions consistent to achieve simultaneous impact on the target. The remaining flight time for the i-th munition is calculated as:

$$t_{go,i} = \frac{\boldsymbol{r}_i}{\dot{\boldsymbol{r}}_i} \tag{4}$$

where r_i is the relative distance and $\dot{r}_i$ is the closing velocity.

The rate of change of the remaining flight time, $t_{go,i}$,reflects the closing acceleration. Its derivation is shown in Equation(5):

$$\dot{t}_{go,i} = \frac{d}{dt}\left(\frac{\boldsymbol{r}_i}{\dot{\boldsymbol{r}}_i}\right) = \frac{\dot{\boldsymbol{r}}_i \cdot \dot{\boldsymbol{r}}_i - \boldsymbol{r}_i \cdot \ddot{\boldsymbol{r}}_i}{\left(\dot{\boldsymbol{r}}_i\right)^2} = 1 - \frac{\ddot{\boldsymbol{r}}_i}{\dot{\boldsymbol{r}}_i} t_{go,i} \text{。} \tag{5}$$

When the target and the munition maintain a constant relative velocity ($\ddot{r} = 0$), $t_{go,i} = 1$. The physical meaning is the natural passage of time; for example, without control, if $t_{go,i} = 10s$, then after 1 second, $t_{go,i}$ becomes 9s.

The difference in the remaining flight time between any two munitions i and j tends to 0 as time t approaches the impact time t_f :

$$\lim_{t\to t_f}\left(t_{go,i}-t_{go,j}\right)=0 \tag{6}$$

Based on this, the cooperative error for the munition can be defined as:

$$e_i=\sum\nolimits_{j=1}^{N}a_{ij}\left(t_{go,i}-t_{go,j}\right) \tag{7}$$

This equation represents the weighted sum of the differences between the remaining flight time of the i-th munition and its neighbors. Since communication quality between munitions may vary, it needs to be considered to improve the cooperative effect. Here, a_{ij} is an element of the adjacency matrix, representing the communication link between munition i and munition j. It is expressed as:

$$a_{ij}=e^{-\gamma\left\|\boldsymbol{r}_i-\boldsymbol{r}_j\right\|^2} \tag{8}$$

where γ is the distance attenuation factor, representing decreasing communication quality with increasing inter-munition distance; $\left\|r_i-r_j\right\|$ is the distance between munitions. This reflects the characteristic that closer munitions have better communication quality. Furthermore, for communication interruption scenarios, the weight is designed as:

$$a_{ij}\left(t\right)=\begin{cases}0.2 & t<5s\\ 0 & t\geq 5s\end{cases} \tag{9}$$

This allows the munition to automatically ignore failed nodes when communication is lost, preventing distortion in the error calculation.

Based on the above, a nonsingular terminal sliding mode surface s_i can be constructed, with the core objective being $s_i=0$ .It can be expressed by Equation(10):

$$s_i=e_i+\beta\int_0^t\left|e_i\right|^{1/2}\operatorname{sgn}\left(e_i\right)d\tau \tag{10}$$

where β is a tuning coefficient used to control the influence of the sliding surface. Differentiating s_i gives:

$$\dot{s}_i=\dot{e}_i+\beta\left|e_i\right|^{1/2}\operatorname{sgn}\left(e_i\right) \tag{11}$$

Setting $\dot{s}_i=0$:

$$\dot{e}_i=-\beta\left|e_i\right|^{1/2}\operatorname{sgn}\left(e_i\right) \tag{12}$$

Solving the differential equation shows the rate of change of error e_i over time. Its solution converges in finite time and strictly converges to 0 after a certain time:

$$e_i\left(t\right)=\begin{cases}\left(e_i\left(0\right)^{1/2}-\dfrac{\beta}{2}t\right)^2\operatorname{sgn}\left(e_i\left(0\right)\right) & t\leq\dfrac{2}{\beta}\left|e_i\left(0\right)\right|^{1/2}\\ 0 & t>\dfrac{2}{\beta}\left|e_i\left(0\right)\right|^{1/2}\end{cases} \tag{13}$$

In actual combat, various disturbances d_i exist which can disrupt the ideal control effect and degrade time synchronization. Although the specific disturbances

are unknown, their absolute value is certainly less than some known upper bound D_i. Therefore, a robust term $u_{r,i}$ is added to the ideal control law $u_{eq,i}$ to resist these disturbances. Its composition can be expressed as:

$$u_{r,i} = k_1 \mathrm{sig}^{1/2}\left(s_i\right) + k_2 \int_0^t \mathrm{sgn}\left(s_i\right) dt \tag{14}$$

In this equation, the first term is a powerful correction term, generating a larger correction force when s_i is large, enabling the cooperative error to decrease rapidly. The second term is a fine-tuning term, representing the accumulation of $\mathrm{sgn}\left(s_i\right)$ over past time. For persistent tiny deviations, the integral term accumulates them; as long as the error direction does not reverse, the corrective force from the integral term gradually increases over time until the tiny deviation is eliminated.

Therefore, the final time cooperative control law is shown in Equation (15):

$$u_{t,i} = k_1 sig^{1/2}\left(\sum\nolimits_{j\in N_i} a_{ij}\left(t_{go,i} - t_{go,j}\right)\right) + k_2 \int_0^t \mathrm{sgn}\left(\sum\nolimits_{j\in N_i} a_{ij}\left(t_{go,i} - t_{go,j}\right)\right) d\tau \tag{15}$$

3.2. Impact Angle Cooperative Controller

The objective of angle cooperation is to enable the selection of the desired impact angle according to the needs when attacking different types of targets. For example, a high impact angle can be adopted for top-attack against armored targets, while a low impact angle can be used for window-penetration attacks against buildings. Different impact angles can also be used against the same target to enhance the attack effect. Similar to the time cooperative controller, for impact angle cooperation, it is desired that the difference between the impact angle ϕ_i of all loitering munitions and the desired impact angle ϕ_d converges to 0 in finite time. It is expressed as:

$$e_{\phi_i} = \phi_i - \phi_d \tag{16}$$

From this, the sliding surface can be established as:

$$s_i = \dot{e}_{\phi_i} + \beta \left|e_{\phi_i}\right|^{\gamma} \mathrm{sgn}\left(e_{\phi_i}\right) \tag{17}$$

where β and γ are sliding surface parameters, with $\beta > 0$ and $0 < \gamma < 1$.

Differentiating Equation (17) gives:

$$\begin{aligned} \dot{s}_i &= \ddot{e}_{\phi_i} + \beta\gamma \left|e_{\phi_i}\right|^{\gamma-1} \dot{e}_{\phi_i} \mathrm{sgn}\left(e_{\phi_i}\right) \\ &= \frac{d}{dt}\left(\dot{\phi}_i - \dot{\phi}_d + \beta \left|e_{\phi_i}\right|^{\gamma} \mathrm{sgn}\left(e_{\phi_i}\right)\right) = \ddot{\phi}_i + \beta\gamma \left|e_{\phi_i}\right|^{\gamma-1} \dot{e}_{\phi_i} \end{aligned} \tag{18}$$

$\ddot{\phi}_i$ can be obtained by differentiating the kinematic formula from Equation(3):

$$\ddot{\phi}_i = \frac{2\dot{\boldsymbol{r}}_i}{\boldsymbol{r}_i}\dot{\phi}_i + \frac{1}{\boldsymbol{r}_i \cos\theta_i}\alpha_{\phi_i} - \frac{1}{\boldsymbol{r}_i}\alpha_{T_\phi} \tag{19}$$

Thus, the impact angle cooperative control law is obtained as:

$$\alpha_{\phi_i} = -r_i \cos\theta_i \left(k_3 s_i + \hat{D}_i \mathrm{sat}\left(s_i\right)\right) \tag{20}$$

In the above equation:

k_3 : Sliding mode control gain, a positive number.

$\hat{D}_i$: Estimated upper bound of the target's maneuvering acceleration (adaptive term).

η : Adaptive gain, a positive number.

$\mathrm{sat}(s_i)$: Saturation function, used to reduce chattering, defined as:

$$\mathrm{sat}(s_i) = \begin{cases} \mathrm{sgn}(s_i) & |s_i| > \Phi \\ \dfrac{s_i}{\Phi} & |s_i| \le \Phi \end{cases} \tag{21}$$

Where Φ is the boundary layer thickness.

When the sliding variable $|s_i|$ increases, the system deviates from the equilibrium point, indicating strong disturbances. $\hat{D}_i$ needs to be increased to enhance robustness. The adaptive law is designed as:

$$\dot{\hat{D}}_i = \eta |s_i| - \sigma \hat{D}_i \tag{22}$$

$\sigma \hat{D}_i$: Leakage term to prevent parameter drift.

3.3. Azimuth Cooperative Controller

3.3.1. Dynamic Azimuth Angle Allocation Strategy

Azimuth cooperation aims to enable several loitering munitions to dynamically disperse around the target during an attack, forming an encirclement to create a containment situation, attack the target more effectively, and prevent the target from escaping. When the target is stationary or moving at low speed, the munitions are distributed omnidirectionally around the target over 360°. As the target's speed increases, the munitions gradually contract to the rear half-plane relative to the target's direction of motion, with the degree of contraction increasing with the target's speed.

To decide whether the munitions are distributed omnidirectionally or contracted to the target's rear, a speed adaptation factor k_v is designed:

$$k_v = \min\left(1, \frac{V_T}{V_{th}}\right) \tag{23}$$

where V_{th} is the speed threshold (taken as 10 m/s), used to distinguish whether the target is in a low-speed motion state. For example, when $V_T = 0$, $k_v = 0$, and the munitions are distributed omnidirectionally around the target; when $V_T > V_{th}$, $k_v = 1$, and the munitions are distributed in a half-plane.

The meanings of the symbols are defined as follows:

V_T : Target velocity.

ψ_T : Target velocity direction angle.

$\alpha_{\max}$: Maximum distribution angle (taken as 60°).

1) Calculate the dynamic distribution angle:

$$\Delta\alpha = 2\alpha_{\max}\left(1-k_v\right)+\alpha_{\max}k_v \tag{24}$$

The meanings of the symbols are defined as follows:

2) Generate the desired azimuth angle:

$$\theta_{d,i} = \psi_T + \alpha_i + \pi \tag{25}$$

The meanings of the symbols are defined as follows:

where the bias angle α_i is:

$$\alpha_i = -\frac{\Delta\alpha}{2}+\frac{\Delta\alpha}{N-1}\left(i-1\right),\ i=1,2,...,N \tag{26}$$

3) Real-time update mechanism:

$$\dot{\theta}_{d,i} = \dot{\psi}_T + \dot{\alpha}_i \tag{27}$$

Since α_i is only updated when N changes or k_v changes, therefore:

$$\dot{\alpha}_i = \begin{cases} \dfrac{d}{dt}\left(-\dfrac{\Delta\alpha}{2}+\dfrac{\Delta\alpha}{N-1}\left(i-1\right)\right) & if\ \dot{k}_v \neq 0\ or\ \dot{N}\neq 0 \\ 0 & otherwise \end{cases} \tag{28}$$

3.3.2. Azimuth Cooperative Control Law

Similar to time and impact angle cooperation, the goal of azimuth cooperation is to make the azimuth angle θ_i of the munition converge to the desired azimuth angle $\theta_{d,i}$ in finite time. Therefore, the design of the azimuth cooperative control law is as follows:

1) Define the azimuth angle error:

$$e_{\theta_i} = \theta_i - \theta_{d,i} \tag{29}$$

2) Nonsingular terminal sliding surface:

$$s_{\theta_i} = \dot{e}_{\theta_i} + \beta_\theta \left|e_{\theta_i}\right|^{\gamma_\theta}\operatorname{sgn}\left(e_{\theta_i}\right) \tag{30}$$

where $\beta_\theta = 1.5$, $\gamma_\theta = 0.8$ (ensuring nonsingularity).

3) Sliding surface derivative derivation:

$$\dot{s}_{\theta_i} = \frac{d}{dt}\left(\dot{\theta}_i - \dot{\theta}_{d,i} + \beta_\theta\gamma_\theta\left|e_{\theta_i}\right|^{\gamma_\theta}\operatorname{sgn}\left(e_{\theta_i}\right)\right) = \ddot{\theta}_i - \ddot{\theta}_{d,i} + \beta_\theta\gamma_\theta\left|e_{\theta_i}\right|^{\gamma_\theta-1}\dot{e}_{\theta_i} \tag{31}$$

4) Azimuth angle dynamics model:

From the missile-target relative kinematics:

$$r_i\ddot{\theta}_i = -\dot{r}_i\dot{\theta}_i + V_M\cos\theta_i\cdot\dot{\theta}_i - V_T\cos\theta_{T,i}\cdot\dot{\theta}_{T,i} + \dot{a}_{\theta_i} \tag{32}$$

5) Control law design:

Let $\dot{s}_{\theta_i} = -k_\theta s_{\theta_i} - \hat{D}_{\theta_i} sat\left(s_{\theta_i}\right)$. Substituting into Eqs. (31) and (32):

$$\ddot{\theta}_i - \ddot{\theta}_{d,i} + \beta_\theta\gamma_\theta\left|e_{\theta_i}\right|^{\gamma_\theta-1}\dot{e}_{\theta_i} = -k_\theta s_{\theta_i} - \hat{D}_{\theta_i}\operatorname{sat}\left(s_{\theta_i}\right) \tag{33}$$

Rearranging gives:

$$\dot{a}_{\theta_i} = r_i \begin{bmatrix} -k_\theta s_{\theta_i} - \hat{D}_{\theta_i} \mathrm{sat}\left(s_{\theta_i}\right) + \ddot{\theta}_{d,i} - \beta_\theta \gamma_\theta \left|e_{\theta_i}\right|^{\gamma_\theta - 1} \dot{e}_{\theta_i} \\ + \dfrac{\dot{r}_i \dot{\theta}_i - V_M \cos\theta_i \cdot \dot{\theta}_i}{r_i} + \dfrac{V_T \cos\theta_{T,i} \cdot \dot{\theta}_{T,i}}{r_i} \end{bmatrix} \tag{34}$$

Incorporating unknown terms into disturbances, the control law can be simplified to:

$$\dot{a}_{\theta_i} = r_i \left(-k_\theta s_{\theta_i} - \hat{D}_{\theta_i} \mathrm{sat}\left(s_{\theta_i}\right) + \ddot{\theta}_{d,i}\right) \tag{35}$$

6) Adaptive law design:

$$\dot{\hat{D}}_{\theta_i} = \eta_\theta \left|s_{\theta_i}\right| - \sigma_\theta \hat{D}_{\theta_i} \tag{36}$$

where $\sigma_\theta > 0$; this is the leakage term to prevent over-estimation.

4 Lyapunov Stability Proof

4.1. Time Cooperation Stability Proof

Theorem 1: The time cooperation subsystem is fixed-time stable.

1) Define the time cooperation error:

$$\delta_i = \sum_{j \in \mathcal{N}_i} a_{ij} \left(t_{go,i} - t_{go,j}\right) \tag{37}$$

2) Error dynamics derivation:

$$\dot{t}_{go,i} = \frac{d}{dt}\left(\frac{r_i}{V_{c,i}}\right) = \frac{\dot{r}_i V_{c,i} - r_i \dot{V}_{c,i}}{V_{c,i}^2} = -1 - \frac{r_i}{V_{c,i}^2} \dot{V}_{c,i} \tag{38}$$

From the control law $\dot{V}_{c,i} = u_{t,i} = k_1 sig^{1/2}\left(\delta_i\right) + k_2 \int_0^t \mathrm{sgn}\left(\delta_i\right) d\tau$:

$$\dot{t}_{go,i} = -1 - \frac{r_i}{V_{c,i}^2}\left(k_1 \left|\delta_i\right|^{1/2} \mathrm{sgn}\left(\delta_i\right) + k_2 \int_0^t \mathrm{sgn}\left(\delta_i\right) d\tau\right) \tag{39}$$

Then the error dynamics:

$$\dot{\delta}_i = \sum_{j \in \mathcal{N}_i} a_{ij} \left(\dot{t}_{go,i} - \dot{t}_{go,j}\right) \tag{40}$$

3) Construct the Lyapunov function:

Using Wang Peng's fixed-time consensus theory [21]:

$$V_t = \frac{1}{2}\delta_i^2 \tag{41}$$

4) Derivative analysis:

$$\dot{V}_t = \delta_i \dot{\delta}_i = \delta_i \sum_{j \in \mathcal{N}_i} a_{ij} \left(\dot{t}_{go,i} - \dot{t}_{go,j}\right) \tag{42}$$

Substituting Equation (27):

$$\dot{V}_t = \delta_i \sum_{j\in\mathcal{N}_i} a_{ij} \begin{bmatrix} \frac{r_j}{V_{c,j}^2}\left(k_1 \left|\delta_j\right|^{1/2} \operatorname{sgn}\left(\delta_j\right) + k_2 \int_0^t \operatorname{sgn}\left(\delta_j\right) d\tau\right) \\ -\frac{r_i}{V_{c,i}^2}\left(k_1 \left|\delta_i\right|^{1/2} \operatorname{sgn}\left(\delta_i\right) + k_2 \int_0^t \operatorname{sgn}\left(\delta_i\right) d\tau\right) \end{bmatrix} \tag{43}$$

Under connected communication topology, the fixed-time convergence condition is satisfied:

$$\dot{V}_t \le -c_1 V_t^{1/2} - c_2 V_t \tag{44}$$

Upper bound of convergence time:

$$T \le \frac{1}{c_2} \ln\left(1 + \frac{c_2}{c_1}\sqrt{2V_t(0)}\right) + \frac{2}{c_1}\sqrt{V_t(0)} \tag{45}$$

Therefore, the time cooperation subsystem is fixed-time stable.

4.2. Impact Angle Cooperation Stability Proof

Theorem 2: The impact angle cooperation subsystem is uniformly ultimately bounded.

1) Construct the Lyapunov function:

$$V = \frac{1}{2} s_i^2 + \frac{1}{2\eta} \tilde{D}_i^2, \tilde{D}_i = D_i - \hat{D}_i \tag{46}$$

D_i :Upper bound of total disturbance, satisfying $\left|d_i\right| \le D_i$.

2) Derivative analysis:

$$\dot{V} = s_i \dot{s}_i + \frac{1}{\eta} \tilde{D}_i \dot{\tilde{D}}_i \tag{47}$$

From $\dot{\tilde{D}}_i = -\dot{\hat{D}}_i$ and Equation(22):

$$\dot{V} = s_i \dot{s}_i + \frac{1}{\eta} \tilde{D}_i \left(\eta \left|s_i\right| - \sigma \hat{D}_i\right) = s_i \dot{s}_i - \tilde{D}_i \left|s_i\right| + \frac{\sigma}{\eta} \tilde{D}_i \hat{D}_i \tag{48}$$

3) Closed-loop dynamics derivation:

Differentiating the kinematic Equation(3):

$$\frac{d}{dt}\left(r_i \dot{\phi}_i \cos\theta_i\right) = -\dot{V}_M \sin\phi_i - V_M \cos\phi_i \cdot \dot{\phi}_i + \dot{V}_T \sin\phi_{T,i} + V_T \cos\phi_{T,i} \cdot \dot{\phi}_{T,i} + \dot{a}_{\phi_i} \tag{49}$$

For low-speed loitering munitions, assume $\dot{V}_M \approx 0, \dot{V}_T \approx 0$:

$$\dot{r}_i \dot{\phi}_i \cos\theta_i + r_i \ddot{\phi}_i \cos\theta_i - r_i \dot{\phi}_i \sin\theta_i \cdot \dot{\theta}_i = -V_M \cos\phi_i \cdot \dot{\phi}_i + V_T \cos\phi_{T,i} \cdot \dot{\phi}_{T,i} + \dot{a}_{\phi_i} \tag{50}$$

$$r_i \cos\theta_i \cdot \ddot{\phi} = -\dot{r}_i \dot{\phi}_i \cos\theta_i + r_i \dot{\phi}_i \sin\theta_i \cdot \dot{\theta}_i - V_M \cos\phi_i \cdot \dot{\phi}_i + V_T \cos\phi_{T,i} \cdot \dot{\phi}_{T,i} + \dot{a}_{\phi_i} \tag{51}$$

4) Substitute the control law:

Substituting the control law (20) into Equation (3) gives:

$$\dot{\phi}_i = \frac{-V_M \sin\phi_i + V_T \sin\phi_{T,i} - r_i \cos\theta_i \left(k_3 s_i + \hat{D}_i \operatorname{sat}\left(s_i\right)\right)}{r_i \cos\theta_i} \tag{52}$$

Substituting this into Equation (51) gives:

$$\begin{aligned}\ddot{\phi}_i &= \frac{1}{r_i\cos\theta_i}\left[-\dot{r}_i\dot{\phi}_i\cos\theta_i + r_i\dot{\phi}\sin\theta_i\cdot\dot{\theta}_i - V_M\cos\phi_i\cdot\dot{\phi} + V_T\cos\phi_{T,i}\cdot\dot{\phi}_{T,i}\right] \\ &+ \frac{d}{dt}\left(-r_i\cos\theta_i\left(k_3 s_i + \hat{D}_i\mathrm{sat}\left(s_i\right)\right)\right)\end{aligned} \tag{53}$$

Expanding the derivative term:

$$\begin{aligned}&\frac{d}{dt}\left(r_i\cos\theta_i\left(k_3 s_i + \hat{D}_i\mathrm{sat}\left(s_i\right)\right)\right) \\ &= \left(\dot{r}_i\cos\theta_i - r_i\sin\theta_i\cdot\dot{\theta}_i\right)\left(k_3 s_i + \hat{D}_i\mathrm{sat}\left(s_i\right)\right) + r_i\cos\theta_i\frac{d}{dt}\left(k_3 s_i + \hat{D}_i\mathrm{sat}\left(s_i\right)\right)\end{aligned} \tag{54}$$

Substituting into Equation(18):

$$\ddot{\phi}_i = f_i\left(\bullet\right) - k_3\dot{s}_i - \hat{D}_i\frac{d}{dt}\mathrm{sat}\left(s_i\right) - \mathrm{sat}\left(s_i\right)\dot{\hat{D}}_i \tag{55}$$

where $f_i\left(\cdot\right)$ contains all known terms.

5) Disturbance separation:

Substituting Equation (55)into the sliding mode dynamics (18):

$$\dot{s}_i = \left[f_i\left(\bullet\right) - k_3\dot{s}_i - \hat{D}_i\frac{d}{dt}\mathrm{sat}\left(s_i\right) - \mathrm{sat}\left(s_i\right)\dot{\hat{D}}_i\right] + \beta\gamma\left|e_{\phi_i}\right|^{\gamma-1}\dot{e}_{\phi_i} \tag{56}$$

where d_i is the total disturbance containing target maneuver and coupling terms.

Rearranging gives:

$$\dot{s}_i = -k_3 s_i - \hat{D}_i\mathrm{sat}\left(s_i\right) + d_i \tag{57}$$

satisfying $\left|d_i\right| \le D_i$.

6) Substitute back into the Lyapunov function:

Substituting Equation (57) into Equation(48):

$$\dot{V} = s_i\left(-k_3 s_i - \hat{D}_i s_i\mathrm{sat}\left(s_i\right) + d_i\right) - \tilde{D}_i\left|s_i\right| + \frac{\sigma}{\eta}\tilde{D}_i\hat{D}_i \tag{58}$$

Expanding:

$$\dot{V} = -k_3 s_i^2 - \hat{D}_i s_i\mathrm{sat}\left(s_i\right) + s_i d_i - \tilde{D}_i\left|s_i\right| + \frac{\sigma}{\eta}\tilde{D}_i\hat{D}_i \tag{59}$$

7) Disturbance upper bound analysis:

Using the inequalities:

$$s_i d_i \le \left|s_i\right|\left|d_i\right| \le \left|s_i\right|D_i - \hat{D}_i\mathrm{sat}\left(s_i\right) \le 0 \tag{60}$$

$$-\tilde{D}_i\left|s_i\right| = -\left(D_i - \hat{D}_i\right)\left|s_i\right| = -D_i\left|s_i\right| + \hat{D}_i\left|s_i\right| \tag{61}$$

Substituting into Equation (59):

$$\dot{V} \le -k_3 s_i^2 + \hat{D}_i\left|s_i\right| + \frac{\sigma}{\eta}\tilde{D}_i\hat{D}_i \tag{62}$$

8) Leakage term handling:

Using the identity:

$$\tilde{D}_i\hat{D}_i = \tilde{D}_i\left(D_i - \tilde{D}_i\right) = D_i\tilde{D}_i - \tilde{D}_i^2 \tag{63}$$

and the inequality:

$$D_i\tilde{D}_i \le \frac{D_i^2}{2} + \frac{\tilde{D}_i^2}{2} \tag{64}$$

yields:

$$\frac{\sigma}{\eta}\tilde{D}_i\hat{D}_i \le \frac{\sigma}{\eta}\left(\frac{D_i^2}{2} + \frac{\tilde{D}_i^2}{2} - \tilde{D}_i^2\right) = \frac{\sigma}{\eta}\left(\frac{D_i^2}{2} - \frac{\tilde{D}_i^2}{2}\right) \tag{65}$$

9) Ultimate boundedness:

Substituting Equation (65) into Equation (62):

$$\dot{V} \le -k_3 s_i^2 + \hat{D}_i\left|s_i\right| + \frac{\sigma}{2\eta}D_i^2 - \frac{\sigma}{2\eta}\tilde{D}_i^2 \tag{66}$$

When $\left|s_i\right| > \frac{\hat{D}_{\max}^2}{k_{3\varepsilon}}$ or $\left|\hat{D}_i\right| > \frac{2D_i^2}{\varepsilon}$

$$\dot{V} \le -\varepsilon V + C \tag{67}$$

where $C = \frac{\sigma}{2\eta}D_i^2$ is a constant.

The system is uniformly ultimately bounded.

4.3. Azimuth Cooperation Stability Proof

Theorem 3: The azimuth cooperation subsystem is globally uniformly ultimately bounded.

1) Construct the Lyapunov function:

$$V_\theta = \frac{1}{2}s_{\theta_i}^2 + \frac{1}{2\eta_\theta}\tilde{D}_{\theta_i}^2, \tilde{D}_{\theta_i} = D_{\theta_i} - \hat{D}_{\theta_i} \tag{68}$$

D_{θ_i} :Upper bound of total disturbance, satisfying $\left|d_{\theta_i}\right| \le D_{\theta_i}$.

2) Derivative and substitute dynamics:

$$\dot{V}_\theta = s_{\theta_i}\dot{s}_{\theta_i} - \frac{1}{\eta_\theta}\tilde{D}_{\theta_i}\dot{\hat{D}}_{\theta_i} \tag{69}$$

From the adaptive law (36):

$$\dot{V}_\theta = s_{\theta_i}\dot{s}_{\theta_i} - \tilde{D}_{\theta_i}\left|s_{\theta_i}\right| + \frac{\sigma_\theta}{\eta_\theta}\tilde{D}_{\theta_i}\hat{D}_{\theta_i} \tag{70}$$

3) Expand $\dot{s}_{\theta_i}$:

Substituting the control law (35) into the dynamics formula (32):

$$\ddot{\theta}_i = \frac{1}{r_i}\left(\dot{r}_i\dot{\theta}_i - V_M\cos\theta_i\cdot\dot{\theta}_i + r_i k_\theta s_{\theta_i} + r_i\hat{D}_{\theta_i}\mathrm{sat}\left(s_{\theta_i}\right) - r_i\ddot{\theta}_{d,i}\right) + \frac{1}{r_i}V_T\cos\theta_{T,i}\cdot\dot{\theta}_{T,i} \tag{71}$$

Substituting into Equation (31):

$$\dot{s}_{\theta_i} = k_\theta s_{\theta_i} + \hat{D}_{\theta_i}\mathrm{sat}\left(s_{\theta_i}\right) + d_{\theta_i} \tag{72}$$

where the total disturbance is:

$$d_{\theta_i} = \frac{\dot{r}_i\dot{\theta}_i - V_M\cos\theta_i\cdot\dot{\theta}_i}{r_i} + \frac{V_T\cos\theta_{T,i}\cdot\dot{\theta}_{T,i}}{r_i} - \beta_\theta\gamma_\theta\left|e_{\theta_i}\right|^{\gamma_\theta-1}\dot{e}_{\theta_i} + \left(\ddot{\theta}_{d,i} - \ddot{\hat{\theta}}_{d,i}\right) \quad (73)$$

4) Substitute back into the Lyapunov derivative:
Substituting Equation (72) into Equation (70):

$$\dot{V}_{\theta_i} = s_{\theta_i}\left(k_\theta s_{\theta_i} + \hat{D}_{\theta_i}s_{\theta_i}\mathrm{sat}\left(s_{\theta_i}\right) + d_{\theta_i}\right) - \tilde{D}_{\theta_i}\left|s_{\theta_i}\right| + \frac{\sigma_\theta}{\eta_\theta}\tilde{D}_{\theta_i}\hat{D}_{\theta_i} \quad (74)$$

Expanding:

$$V_{\theta_i} = k_\theta s_{\theta_i}^2 + \hat{D}_{\theta_i}s_{\theta_i}\mathrm{sat}\left(s_{\theta_i}\right) + s_{\theta_i}d_{\theta_i} - \tilde{D}_{\theta_i}\left|s_{\theta_i}\right| + \frac{\sigma_\theta}{\eta_\theta}\tilde{D}_{\theta_i}\hat{D}_{\theta_i} \quad (75)$$

5) Disturbance upper bound analysis:
Using the inequalities:

$$s_{\theta_i}d_{\theta_i} \le \left|s_{\theta_i}\right|\left|d_{\theta_i}\right| \le \left|s_{\theta_i}\right|D_{\theta_i} \quad (76)$$

$$\hat{D}_{\theta_i}s_{\theta_i}\mathrm{sat}\left(s_{\theta_i}\right) \le \hat{D}_{\theta_i}\left|s_{\theta_i}\right| \quad (77)$$

$$-\tilde{D}_{\theta_i}\left|s_{\theta_i}\right| = -\left(D_{\theta_i} - \hat{D}_{\theta_i}\right)\left|s_{\theta_i}\right| = -D_{\theta_i}\left|s_{\theta_i}\right| + \hat{D}_{\theta_i}\left|s_{\theta_i}\right| \quad (78)$$

Substituting into Equation (75):

$$\dot{V}_\theta \le -k_\theta s_{\theta_i}^2 + 2\hat{D}_{\theta_i}\left|s_{\theta_i}\right| + \frac{\sigma_\theta}{\eta_\theta}\tilde{D}_{\theta_i}\hat{D}_{\theta_i} \quad (79)$$

6) Leakage term handling:
Using the identity:

$$\tilde{D}_{\theta_i}\hat{D}_{\theta_i} = \tilde{D}_{\theta_i}\left(D_{\theta_i} - \tilde{D}_{\theta_i}\right) = D_{\theta_i}\tilde{D}_{\theta_i} - \tilde{D}_{\theta_i}^2 \quad (80)$$

and the inequality:

$$D_{\theta_i}\tilde{D}_{\theta_i} \le \frac{D_{\theta_i}^2}{2} + \frac{\tilde{D}_{\theta_i}^2}{2} \quad (81)$$

yields:

$$\frac{\sigma_\theta}{\eta_\theta}\tilde{D}_{\theta_i}\hat{D}_{\theta_i} \le \frac{\sigma_\theta}{\eta_\theta}\left(-\frac{1}{2}\tilde{D}_{\theta_i}^2 + \frac{1}{2}D_{\theta_i}^2\right) \quad (82)$$

7) Ultimate boundedness proof:
Substituting Equation (82) into Equation (79):

$$\dot{V}_\theta \le -\left(\left|k_\theta\right|s_{\theta_i}^2 + \frac{\sigma_\theta}{2\eta_\theta}\tilde{D}_{\theta_i}^2\right) + 2\hat{D}_{\theta_i}\left|s_{\theta_i}\right| + \frac{\sigma_\theta}{2\eta_\theta}D_{\theta_i}^2 \quad (83)$$

When $\left|s_{\theta_i}\right| > \frac{4\hat{D}_{\max}^2}{\varepsilon}$ or $\left|\tilde{D}_{\theta_i}\right| > \frac{2D_{\theta_i}^2}{\varepsilon}$:

$$\dot{V}_\theta \le -\varepsilon V_\theta + C \quad (84)$$

where $C = \frac{\sigma\theta}{2\eta\theta}D_{\theta_i}^2$ is a constant.

Therefore, the system is uniformly ultimately bounded.

5 Simulation Experiments

To validate the effectiveness of the cooperative guidance law, simulation programs were developed based on MATLAB for digital simulation experiments.

In terms of simulation system design, targeted adjustments were made to account for the characteristics of the loitering munitions, such as the use of image guidance and Bank-to-Turn (BTT) coordinated turn control. The simulations modeled the limitations of the loitering munition seeker's field of view and effective detection range. During turning maneuvers, the munitions follow Dubins paths under the constraint of a minimum turning radius.

The simulations were conducted using a Monte Carlo method with multiple runs. The target and loitering munitions were initially randomly distributed within a 2000m × 2000m area. The number of loitering munitions can be customized. The target maneuvers by moving 200 meters and randomly turning 60 degrees left or right, simulating evasive actions. The simulation time step was set to 0.01s. The basic parameters of the loitering munitions and the target are shown in Table 1.

Table 1. Loitering Munition and Target Parameters

Parameters	Value	Unit
Target Speed	0	m/s
Target Initial Position	(0,0)	
Target Single Movement Distance	200	m
Target Turning Angle	60	°
Loitering Munition Maximum Speed	60	m/s
Loitering Munition Cluster Initial Center	(-700,700)	
Loitering Munition Turning Radius	75	m

5.1. Low-Speed Moving Target

Three loitering munitions were used to attack a target moving at 5m/s. The simulation results are as follows.

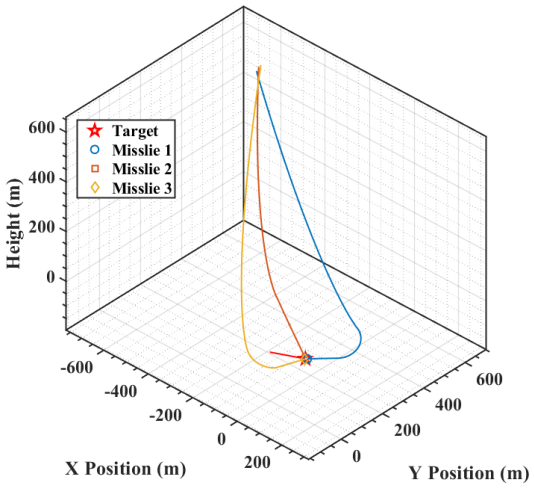

(a) 3D Trajectory Plot

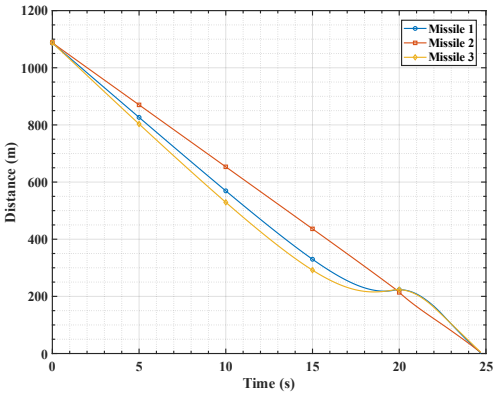

(b) Missile-Target Distance vs. Time

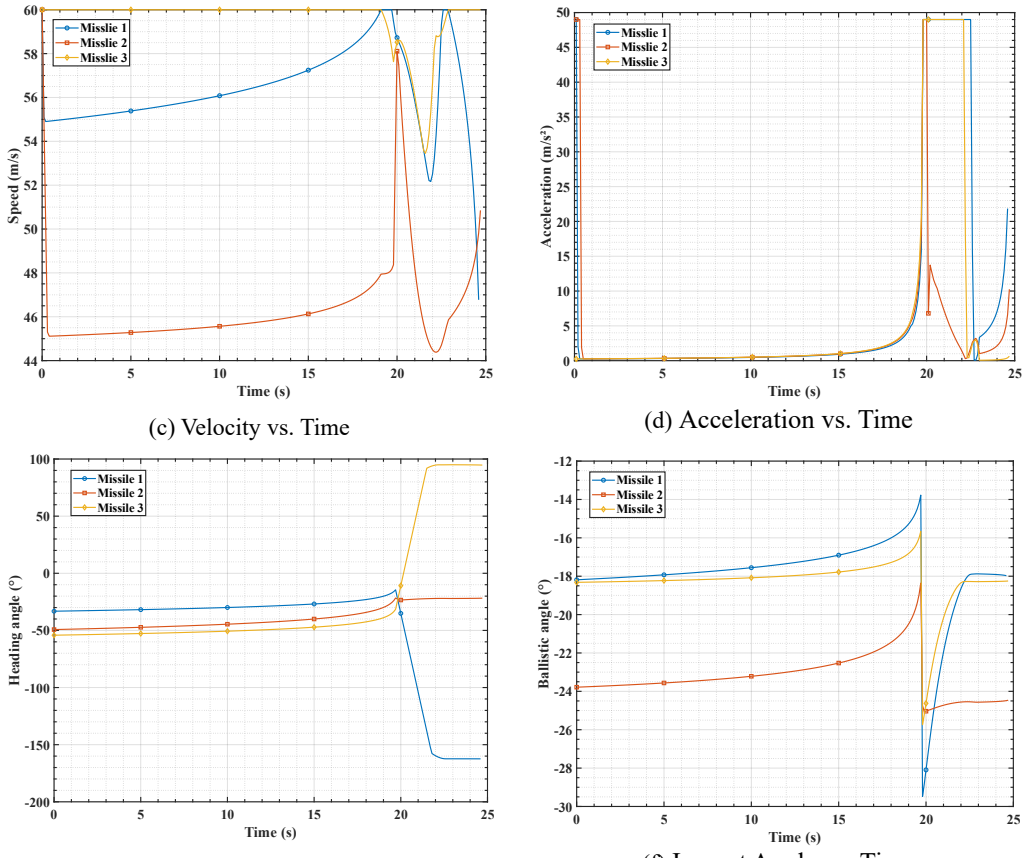

(c) Velocity vs. Time

(d) Acceleration vs. Time

(e) Azimuth Angle vs. Time

(f) Impact Angle vs. Time

Figure 1. Three Munitions vs. Low-Speed Target: Simulation Results

The impact times of the loitering munitions are shown in Table 2:

Table 2. Loitering Munition Time-of-Attack Parameters

Loitering Munition No.	Impact Time (s)
1	24.58
2	24.61
3	24.60

From the simulation results, it can be observed that when attacking a low-speed moving target, the loitering munitions are approximately uniformly distributed around the target, launching an omnidirectional attack. Each munition automatically selects an appropriate impact angle based on its own state. The acceleration of the loitering munitions is limited to within 5g, and the standard deviation of the impact time is 0.01247s.

5.2. Medium-Speed Moving Target

The number of individuals in the loitering munition cluster and the target's speed were increased. Five loitering munitions were used to attack a target moving at 10m/s. The simulation results are as follows.

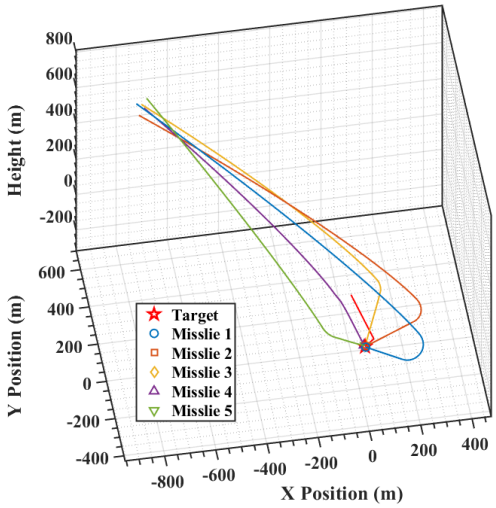

(a) 3D Trajectory Plot

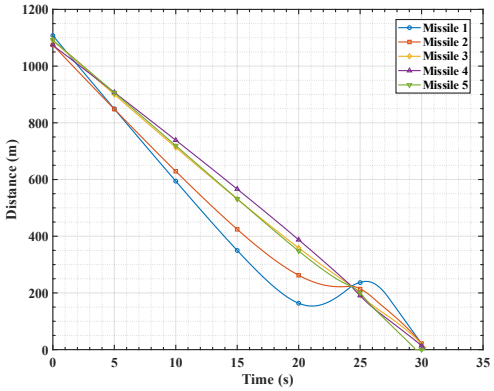

(b) Missile-Target Distance vs. Time

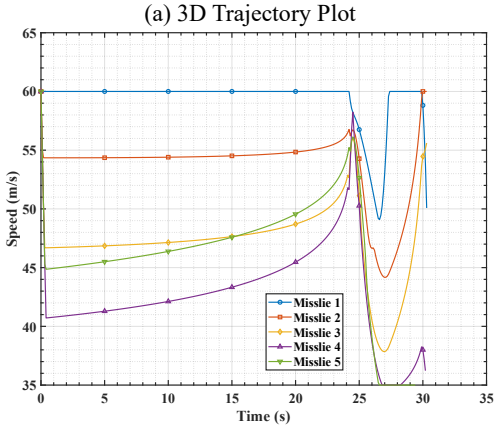

(c) Velocity vs. Time

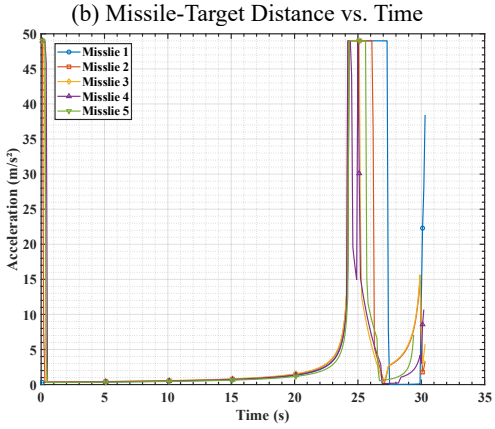

(d) Acceleration vs. Time

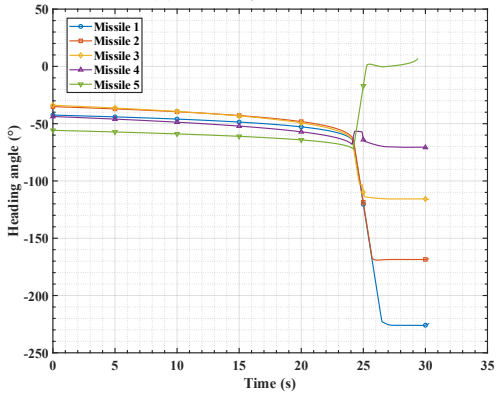

(e) Azimuth Angle vs. Time

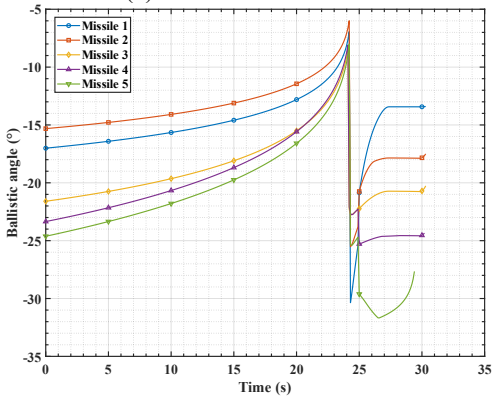

(f) Impact Angle vs. Time

Figure 2. Five Munitions vs. Medium-Speed Target: Simulation Results

Table 3. Loitering Munition Time-of-Attack Parameters

Loitering Munition No.	Impact Time (s)
1	30.21
2	30.20
3	30.22
4	30.18
5	29.31

As the target's speed increases, the distribution of the munitions' attack azimuth begins to contract towards the rear of the target's direction of motion, showing a greater tendency to adopt a pursuit strategy. Each munition adjusts its flight speed in real time based on the remaining time-to-go to achieve time coordination. The standard deviation of the impact time is 0.35725s.

5.3. High-Speed Moving Target

To verify the performance of a larger-scale cluster, eight loitering munitions were used to attack a target moving at 20m/s. The simulation results are as follows.

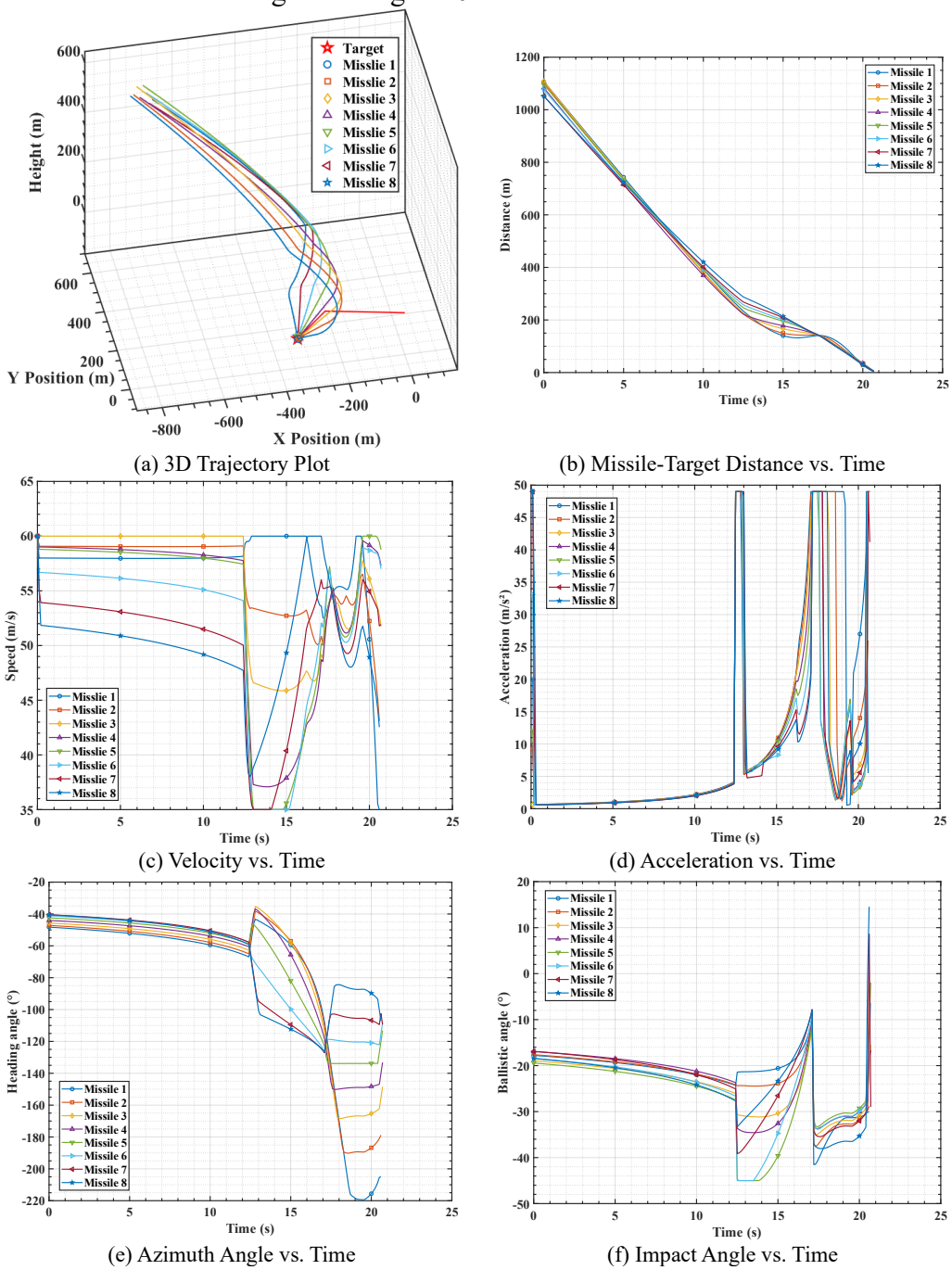

(a) 3D Trajectory Plot

(b) Missile-Target Distance vs. Time

(c) Velocity vs. Time

(d) Acceleration vs. Time

(e) Azimuth Angle vs. Time

(f) Impact Angle vs. Time

Figure 3. Eight Munitions vs. High-Speed Target: Simulation Results

Table 4. Loitering Munition Time-of-Attack Parameters

Loitering Munition No.	Impact Time (s)
1	20.56
2	20.55
3	20.60
4	20.61
5	20.59
6	20.57
7	20.53
8	20.62

Table 5. Terminal Impact Angle Parameters for Loitering Munitions

Loitering Munition No.	Impact Angle (°)
1	-30.053
2	-28.863
3	-15.540
4	-16.685
5	-1.947
6	-6.363
7	-28.993
8	14.540

When the target's speed further increases, the attack azimuth sector contracts even more to adopt a tail-chase method, avoiding misses caused by insufficient maneuverability of the munitions in a head-on engagement. The maximum terminal impact angle is 30.053°, and multiple munitions have different impact angles, enabling attacks on the top and rear weak armor of armored vehicles. The standard deviation of the impact time is 0.02934s.

6 Conclusion

This paper focuses on the multi-constraint guidance problem in cooperative strikes by loitering munitions. A distributed spatio-temporal cooperative guidance law based on adaptive sliding mode control was designed and validated. Through theoretical derivation and numerical simulation, the following conclusions are drawn:

1) The proposed guidance law can effectively achieve cooperative control of multiple munitions in terms of impact time, impact angle, and attack azimuth. It demonstrates good convergence and stability under different target speed conditions.

2) The dynamic azimuth allocation strategy can adaptively adjust the attack formation based on target speed. It achieves omnidirectional encirclement at low speeds and automatically switches to rear half-plane pursuit at high speeds, significantly enhancing the encirclement capability and tactical adaptability against maneuvering targets.

3) Stability analysis based on Lyapunov theory shows that the time-cooperative subsystem has fixed-time convergence characteristics, while the impact angle and azimuth cooperative subsystems are uniformly ultimately bounded. The overall system exhibits strong robustness.

4) Simulation results show that the overload of the loitering munitions during the control process can be limited to within 5g, meeting practical engineering constraints. The small standard deviation of the impact time (maximum of 0.357s) verifies the effectiveness and practicality of the guidance law.

This research provides a feasible guidance solution for cooperative strikes by loitering munition clusters, particularly suitable for multi-azimuth cooperative attack scenarios against ground maneuvering targets, and possesses certain military application value. Future work could further consider optimizing the guidance law under practical constraints such as communication delays, topology switching, and obstacle avoidance.

References

[1] Sheng, D., Analysis of the development and combat application of loitering missiles, *Journal of Projectiles, Rockets, Missiles and Guidance*, **45** (03) (2025), 323-329.

[2] Liu, S.; Xu, X.; Huang, W.; Yan, B.; Lin, Z.; Ma, W., Development and Key Technologies Outlook of Foreign Multi-Missile Collaborative Projects, *Aero Weaponry,* **31** (06) (2024), 1-13.

[3] Zhou, M.; Wang, Y.; Guo, J.; Lu, X., A Survey of Multi-Missile Cooperative Terminal Guidance, *Aero Weaponry*, **30** (04) (2023), 17-25.

[4] Zhao, J.; Wang, R.; Li, X.; Zhang, D., Cooperative attack strategy during the terminal guidance phase for loitering munitions based on impact angle and impact time constraints, *Journal of Northwestern Polytechnical University*, **42** (03) (2024), 386-395. https://doi.org/10.1051/jnwpu/20244230386

[5] Chen, W.; He, F.; Wang, Z.; Dong, L., Cooperative Optimal Predictive Guidance Law Considering Terminal Impingement Angle Constraints, *Fire Control & Command Control,* **50** (01) (2025), 95-103+112.

[6] Li, H.; Wang, J.; Zhang, R.; Song, F., Underactuated Three-dimensional Cooperative Guidance Law with Time and Angle Constraints, *Journal of Astronautics*, **45** (10) (2024), 1633-1644.

[7] Guo, Z.; Li, G.; Xiong, H.; Wu, Y., Cooperative Guidance Method with Impact Time and Area Sealing, *Journal of System Simulation*, (2025), 1-10. https://link.cnki.net/urlid/11.3092.v.20250717.1633.003

[8] Ma, Z.; Zhang, Z.; Shi, Z.; Song, T.; Xie, Z., Research on Three-dimensional Guidance Law for Cooperative Attack Considering Avoidance Zone and Line of Sight Angle Constraints, *Journal of Projectiles, Rockets, Missiles and Guidance*, **30** (04) (2023), 17-25.

[9] Wang, X.; Lu, H.; Huang, X., Three-dimensional terminal angle constraint finite-time dual-layer guidance law with autopilot dynamics, *Aerospace Science and Technology*, **116** (2021), 106818. https://doi.org/10.1016/j.ast.2021.106818

[10] Polyakov, A., Nonlinear feedback design for fixed-time stabilization of linear control systems, *IEEE Transactions on Automatic Control*, 57 (8) (2011), 2106-2110. https://doi.org/10.1109/tac.2011.2179869

[11] Lin, H.; Liu, B.; Pan, T.; Kong, Z., Design of a Sliding Mode Cooperative Guidance Law against Maneuvering Target, *Modern Defense Technology*, (2025), 1-10. https://link.cnki.net/urlid/11.3019.tj.20250312.0938.006

[12] Huang, S.; Du, Y.; Liu, Y.; Wang, Y.; Liu, W., Adaptive sliding cooperative terminal guidance with finite-time convergence, *Systems Engineering and Electronics*, **47** (03) (2025), 961-969.

[13] Chang, Y.; Wang, X.; Li, G., Prescribed-time Convergent Cooperative Guidance Method with Impact Time and Angle Constraints, *Journal of Beijing University of Aeronautics and Astronautics*, (2025), 1-14. https://doi.org/10.13700/j.bh.1001-5965.2024.0395

[14] Si, Y.; Xiong, H.; Song, X.; Zong, R., Three dimensional guidance law for cooperative operation based on adaptive terminal sliding mode, *Acta Aeronautica et Astronautica Sinica*, **41** (S1) (2020), 99-109. https://doi.org/10.1016/j.cja.2015.12.012

[15] Wang, Y.; Wang, W.; Lin, S.; Yang, J.; Wang, S.; Yin, Z., Three-dimensional Adaptive Sliding Mode Cooperative Guidance Law with Impact Time and Angle Constraints, *Acta Armamentarii*, **44** (09) (2023), 2778-2790.

[16] Gao, Q.; Yuan, Y.; Yuan, H.; Wang, M., Cooperative Differential Games Guidance Laws with Multiple Constraints for Intercepting Maneuvering and Varying-speed Targets, *Journal of Astronautics*, **45** (12) (2024), 1944-1958.

[17] Yuan, Y.; Wang, Z.; Guo, L., Event-triggered strategy design for discrete-time nonlinear quadratic games with disturbance compensations: The noncooperative case, *IEEE Transactions on Systems, Man, and Cybernetics: Systems,* **48** (11) (2018), 1885-1896. https://doi.org/10.1109/tsmc.2017.2704278

[18] Chen, S.; Yang, Y.; Ma, D., Cooperative guidance law with impact angle coordination: A Nash approach, *IEEE Transactions on Aerospace and Electronic Systems*, **58** (5) (2022), 3924-3931. https://doi.org/10.1109/taes.2021.3134998

[19] Yang, Z.; Zhang, S.; Zhang, C.; Wang, H.; Zhao, M., Missile anti-collision c ooperative guidance based on differential game, *Systems Engineering and Ele ctronics,* (2025) 1-11. https://link.cnki.net/urlid/11.2422.TN.20250102.1104. 006

[20] Zhan, Y.; Li, S.; Zhou, D.; Wu, S., Three-dimensional Multi-missile Game Guidance Law based on Cooperative Estimation, *Journal of Astronautics*, **45** (09) (2024), 1467-1480.

[21] Wang, P.; He, Z.; Li, J.; Li, H.; Geng, B.; Fan, W., Event-Triggered Fixed-Time Cooperative Guidance Law Against Maneuvering Target, *Transactions of Beijing Institute of Technology*, **44** (10) (2024), 1040-1050.

Received: August 31, 2025; Published: September 15, 2025